Permeability Measurement and Numerical Modeling for Refractory Porous Materials

X. Chen
MDSHA, Cockeysville, Maryland

D. Penumadu
University of Tennessee, Knoxville, Tennessee

ABSTRACT

The transport properties of the ceramic based refractory coating to allow proper permeation of degradation products during the pyrolysis of expanded polystyrene (EPS) foam in Lost Foam Casting (LFC) have an important influence on the success of the casting process. This paper proposes a new apparatus to evaluate the permeability of the refractory coatings in a relatively large differential pressure range that is expected during the casting process. A number of commercial coatings currently used in major LFC foundries are evaluated, and the results show significant differences in their transport properties. The proposed interpretation method of measured gas flow data is considered the "slippage" and inertia effects that occur in measuring gas permeability. It is found that special care should be taken to measure the coating permeability in a large velocity range. Comparisons of test results from this new device are made to the widely used General Motors (GM-hereafter referenced as Foundry A) Perm-meter. The proposed measurement technique is more reliable to evaluate the permeability of the refractory LFC coatings in a large velocity range and considers inertia effects. A procedure using three-dimensional computational fluid dynamics code (FLOW3D) is developed to simulate experimental gas flow data for solving complex boundary value problems that use these coatings.

Key Words: Lost Foam Casting, porous material, permeability, gas flow

INTRODUCTION

Lost Foam Casting (LFC) is a relatively new technique used to produce metal casting products in near net-shape. This process involves pouring molten metal into an expanded polystyrene foam pattern that is coated using refractory slurry and surrounded by un-bonded foundry sand. The temperature of the molten metal is significantly higher than the degradation temperature of the expanded polystyrene foam pattern and results in pyrolysis generating gas and liquid by-products.[1,2] These degradation products should escape the pore network of thin refractory coating into surrounding sand pores and yield a cavity that is an exact replica of the casting shape. The metal then replaces the shape of the polystyrene foam pattern to yield the complex shaped casting in near net-shape. Refractory coating is very critical for successful outcome and one of its important properties is associated with transport properties of gas (predominantly styrene). Un-bonded granular sand or mullite is compacted around the foam pattern, providing support for the coated foam pattern by keeping the pattern in place during the metal pouring and filling process.

Research[3-9] has found that most defects observed in the metal casting obtained from the LFC process are related to the mechanism of how the gas and liquid pyrolysis products of EPS foam escape during the metal filling process. This mechanism requires that the refractory coating have certain permeable characteristics to allow the escape of thermally degraded polystyrene products. High permeability coating will reduce the time required for eliminating EPS degradation products and will increase the metal fill velocity, often leading to blister and fold defects. Low permeability coating will slow down the metal velocity, which causes the molten metal to lose the adequate thermal energy for complete pyrolysis, traps the liquid and solid polystyrene, and leads to misrun or partial fill. Sands et al.,[10] demonstrated the influence of coating permeability on mold filling in the LFC process by changing coating thickness. It showed that mold filling times decreased with the permeability of the coatings. From a practical point of view, the gas permeability of the refractory coatings has been one of the most critical factors in the LFC process for casting quality control.

With an increasing interest in evaluating the role of coating transport properties, attempts were made in the foundry industry to determine the permeability of a given refractory based coating. Goria[3] evaluated permeability by measuring "flow time" to reach an equilibrium state between the applied pressure and the atmospheric pressure. Tseng and Askeland[11] used a modified steel cylinder and a standard permeability meter that is often used to characterize sand cores in the foundry industry to

evaluate the permeability of the coating by measuring flow through a coated filter paper for a fixed differential pressure. Ravindran et al.,[12] assessed the permeability of the coating by measuring the flow rate of air through the coated wafers at a constant vacuum. FOUNDRY A measured coating permeability by using the existing Perm-meter used for greensand and evaluating the flow rate of air through a coated stainless steel mesh (#100 sieve screen) at constant pressure.[13] Littleton et al.,[6] calculated the permeability coefficient by manually measuring gas flow rates at various pressures.

These methods provided solutions to qualitatively, and to a limited extent quantitatively, describe the gas transport properties of the LFC coatings. Some of the limitations of past research include the difficulty of interpretation, such as "flow time," and poor repeatability of the experimental measurements in appropriate pressure ranges. FOUNDRY A perm-meter does not account for the coating thickness in its empirical measurement number called Perm value (typically in the range of 0 to 20) and cannot account for different coating thickness values. In addition, it may not be suitable to predict the coating permeability at various pressures using the results from a single point measurement system, as will be demonstrated later in this paper. Moreover, none of the past methods mentioned above have considered that gas is a compressible medium and do not consider the possibility of "gas slippage" flow and inertia flow. Considering the fact that one of the important quality control tools for LFC coating is based primarily on permeability measurements, it is important to develop and validate the use of a measurement technique that is robust from instrumentation and interpretation points of view.

This paper proposes a new approach for investigating coating permeability by considering the compressible property of gas and the effect of inertia in a relatively large pressure range using a fully automated system. In addition, a computational fluid dynamics model in Flow 3D is proposed to simulate gas flowing through LFC coatings, which demonstrates that the parameters obtained from proposed approach can be numerically incorporated into commercial CFD software. This would facilitate the future constitutive modeling of refractory coating for simulating Lost Foam Casting as a boundary value problem.

ANALYSIS BACKGROUND

A standard approach to characterize the permeability of porous materials is to use Darcy's law (Equation 1), which relates volumetric flow and pressure gradient with properties of the fluid and porous materials.

$$Q = -\frac{kA}{\mu}\frac{dP}{L}$$
Equation 1

Q -- volumetric flow
A -- cross-sectional area
μ -- viscosity of the fluid
$\dfrac{dP}{L}$ -- pressure gradient
L -- coating thickness
k -- Darcian permeability coefficient

The Darcian permeability coefficient k indicates the capability of the porous medium to transmit fluids. It will be possible to predict flow behavior of any liquid through the porous medium once the Darcian permeability coefficient k can be measured or calculated.

If considering gas as a compressible fluid, the Darcy law (Equation 1) can be rewritten as

$$Q = \frac{kA}{\mu}\frac{P_i^2 - P_0^2}{2PL}$$
Equation 2

or

$$\frac{P_i^2 - P_0^2}{2PL} = \frac{\mu}{k} \cdot v_s$$
Equation 3

P_i -- pressure at the sample entrance
P_o -- pressure at the sample exit
P -- fluid pressure at which Q and μ are measured or calculated

$\dfrac{P_i^2 - P_0^2}{2PL}$ -- pressure gradient

v_s -- velocity (Q divided by area)

Theoretically, the permeability coefficient only depends on the porous medium's properties. However, careful analysis of past literature reports that permeability measurements using compressible gases may give different permeability coefficients at various pressures due to inertia effects as described below. Darcian permeability k may be extremely high at low pressures. This phenomenon is caused by "slippage" in the gas flow, which was first investigated by Klinkenberg in 1941.[14] At low pressures, the molecules in the gas have few collisions between each other and the passages in the porous media. The molecules "slip" in the passages, so that gas can easily pass through the channels in the porous medium. This process is also related to the size of the gas molecule. Small molecules in the gas will exhibit significantly more slippage than larger gas molecules at similar pressures. This effect will become more pronounced when the diameter of the passages is close to the mean free path of the gas molecules. At high pressures, the turbulent and inertia flow become more dominant so that Darcy's law is no longer valid. Forchheimer's equation[15] is introduced here, which includes parabolic parts in the equation by considering the influence of inertia and turbulence. Forchheimer's equation is normally written as

$$\frac{P_i^2 - P_0^2}{2PL} = \frac{\mu}{k_1} v_s + \frac{\rho}{k_2} v_s^2 \qquad\qquad \text{Equation 4}$$

where ρ is the fluid density; constant k1 and k2 are the Darcian (viscous) permeability and non-Darcian (inertia) permeability, respectively; vs is the fluid velocity, calculated by dividing the exiting volumetric flow rate Q by the cross-sectional area A. Equation 4 is not a pure empirical equation. It can be theoretically derived by appropriately averaging the Navier-Stockes equations.[16] The first term in Equation 4 represents viscous energy losses, while the second term represents the inertia effects.

A dimensionless number, the Reynolds number (Re), representing the ratio of inertia to viscous forces, is widely used as a criterion to distinguish between laminar flow and turbulent flow. The Reynolds number is written as

$$\text{Re} = \frac{v \cdot \rho \cdot \delta}{\mu} \qquad\qquad \text{Equation 5}$$

where v is the velocity, ρ the density, μ the viscosity of the fluid, and δ a diameter associated with the porous medium (average pore diameter).[17] Darcy's law is valid only at a low Reynolds number. The upper limit is at a value of Re between 1 and 10.[16] At a high Reynolds number, the deviation from Darcy's law will be observed. Research[16] has shown that the deviation from Darcy's law (which occurs at Re = 1 ~10) cannot be attributed to turbulence, and the inertia forces are more appropriate to explain the deviation.

EXPERIMENTS

SAMPLE PREPARATION
For this study, five different types of Lost Foam Casting refractory coating slurries (A ~ E) were investigated. These slurries were produced for two major automotive Powertrain LFC foundries by three commercial suppliers. In order to investigate the dilution effects, a synthetic coating F was obtained by adding 5 percent of water by volume to a commercial coating D. Similarly, the synthetic coating G was obtained by adding 5 percent of water by volume to another commercial coating E. The information about the coating samples A ~ G used in this study is listed in Table 1. Malvern Mastersizer S, which employs the Laser Light Scattering technique, was utilized to measure the mean equivalent volume-based diameters.

Table 1. Coating Samples Used in This Study

Coating ID	Bulk Density (g/cc)	Percentage Of solids	Mean Diameter (Based on volume distribution using Laser Light Scattering) (um)
A	1.46	52.7%	62.6
B	1.33	42.71%	27.1
C	1.37	46.5%	33.4
D	1.42	50.53%	50.6
E	1.55	62.73%	33.3
F	1.4	48.81%	50.6
G	1.53	60.77%	33.4

The coating samples were obtained by dipping a 100x100 stainless steel mesh disc of 65mm diameter into the coating slurries, whose rheological properties were well-controlled. The steel mesh has a very high permeability, which will not affect the measuring results for the coating permeability. The steel mesh disc with very large pore size acts as a supporting medium for the coating to bond and dry without affecting the permeability. The dipped coating discs were then dried at room temperature. After drying, the thickness of each coating was measured by a micrometer with good resolution. In order to investigate the effects of drying on the coating permeability, two sets of coating D and E were prepared and dried using air (25°C) or oven drying (60°C). For oven-dried samples, after removal of the disc from the coating slurry container, these samples were initially dried at room temperature for 10 – 15 minutes before being placed in a drying oven as suggested in previous research.[13]

These coating samples were supplied by LFC foundries to the authors with the permeability measured using a FOUNDRY A Perm-meter for comparison. The permeability of these samples was also assessed in this study to investigate the relationship between the FOUNDRY A perm-meter reading and the permeability coefficient obtained from Darcy's law and Forchheimer's equation as obtained in this research.

PORTABLE UTK PERM-METER DEVELOPMENT
Testing of all the samples was conducted in a Capillary Flow Porometer manufactured by Porous Material, Inc., and a portable Perm-meter (UTK Perm-meter) (Figure 1) developed by the authors of this paper.
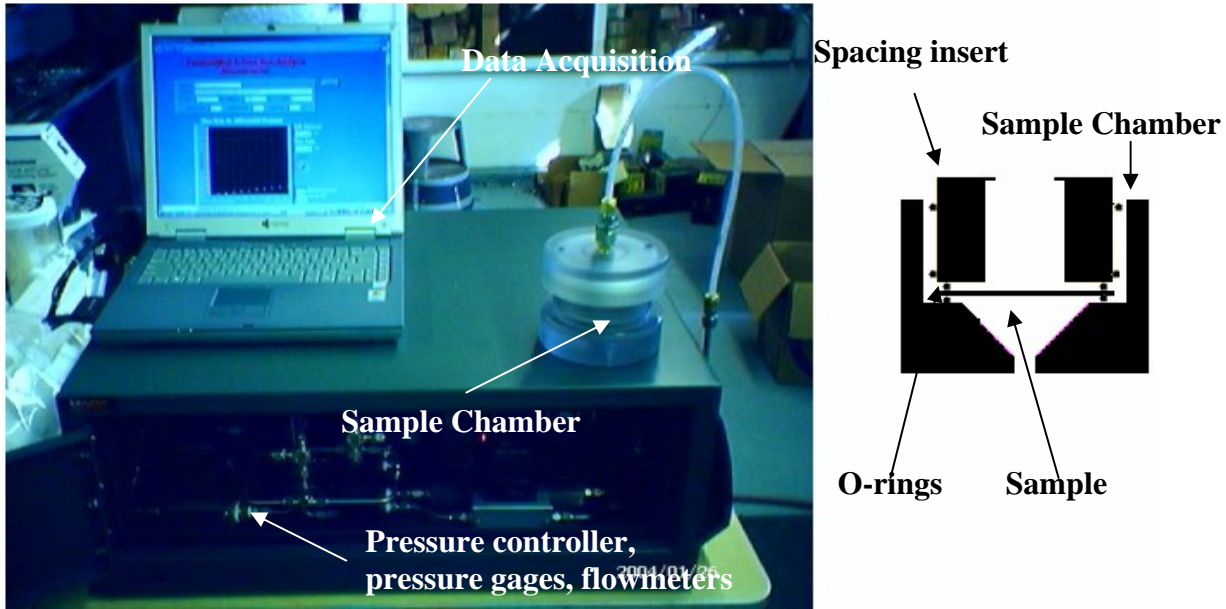
Testing of all the samples was conducted in a Capillary Flow Porometer manufactured by Porous Material, Inc., and a portable Perm-meter (UTK Perm-meter) (Figure 1) developed by the authors of this paper.

Figure 1: UTK Perm-meter System

The Capillary Flow Porometer and UTK Perm-meter have similar concepts and can measure the microstructure information of the porous medium[18] in addition to the global permeability. The UTK perm-meter is a fully computer-controlled device comprised of two pressure controllers, one pressure gage, two flowmeters, three solenoid valves, one relay controller, sample chamber, and data acquisition system as illustrated in Figure 2.
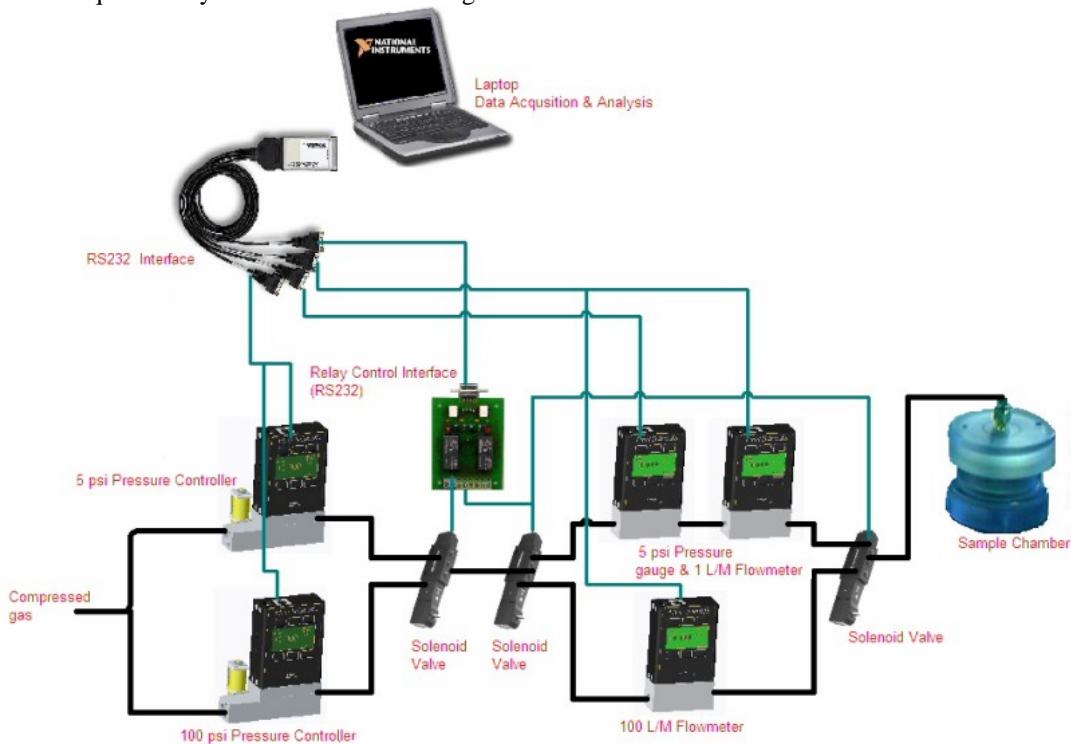
Figure 2: Schematics of UTK Perm-meter System

The software utilized in this perm-meter was developed in the graphic programming language LabVIEW Express 7. After being assigned a starting pressure, ending pressure, and target data points in between the range, the software will automatically control the pressure controller to increase pressure and measure the flow rate. The pressure and flow rate

information will be recorded and plotted on the screen once steady flow is achieved. The UTK Perm-meter can precisely control pressure from 0.07 kPa to 700 kPa and measure the flow from 0.01 liter/min to 100 liter/min. The coating sample is placed in the sample chamber (Figure 1), in which o-rings constrain the gas to flow up and out of the chamber. Thus the flow cross-sectional area is always known and avoids gas flow due to in-plane transmission.

EXPERIMENTAL PROCEDURE AND DATA ANALYSIS

The permeability of refractory LFC coatings was measured at room temperature using the apparatus previously described. The applied differential pressure (Pi-Po) was in the range of 0 – 700 kPa. All the data were acquired electronically at one-second intervals throughout the experiment. The Pi, Po, and Q values were recorded at a steady flow. Permeability coefficients were obtained by fitting experimental data through the least squares method to Equations 3 and 4.

NUMERICAL MODELING OF GAS FLOW THROUGH LFC COATING

Through the efforts of many researchers in Lost Foam Casting, the formation mechanism of commonly observed defects has been established to rate the metal casting quality and classify the reject castings. However, there are still many unknown issues in the LFC process that affect casting quality. For example, the mechanism of mass and heat transfer between the molten metal, degraded liquid/gas monomer/dimmers/trimmers, coating, and unbonded sand is not well understood. Ongoing research and new experiments aimed at exploring the physical mechanisms behind the LFC process are ongoing.[19-21] Such experiments are very time consuming and multivariate. In addition, because of complicated casting conditions such as gating, pouring temperatures, coating refractory and transport properties, and compaction and thermal properties of unbonded sand, it is very difficult to control the casting conditions as accurately as designed. In order to get a reasonably good casting quality of newly designed products, extensive trial-and-error procedures are needed before production. The trial-and-error method used to determine casting conditions can be very costly and may not always yield successful results.[22] This demonstrates the need for computer simulation to reduce the time and expense of determining the casting conditions and to explore the physical mechanism behind the LFC process.

Wang and Paul[22] developed a finite difference method (FDM) program to simulate fluid flow and heat transfer during mold filling for the EPC process in 3D geometry. The decomposition rate of the foam pattern was expressed as a function of temperature and pressure at the metal-pattern interface. Solidification and other useful information were obtained through the simulation. Hirt and Barkhudarov[23] simulated the LFC process to track defects using a commercial Computation Fluid Dynamic (CFD) software Flow 3D. The LFC model in Flow 3D considered the foam as a special kind of obstacle that can prevent the flow of metal unless it is heated sufficiently to lose its strength, which suggested that the displacement of foam by metal was controlled by the heat transfer mechanism instead of pressure or inertia of metal. This simulation considered the effects of coating permeability by changing the heat transfer coefficient at the interface of metal and foam. However, there is a need for realistic constitutive modeling of foam and coating and a multi-phase computational fluid dynamic code to realistically model the observed casting degradation experiments from real time X-ray and neutron radiography.

In this study, a baffle flow losses model in Flow 3D was used to simulate the gas flow through LFC coating. At a constant flow rate, the pressure gradient across the coating can be modeled as

$$\Delta p = \rho \cdot (KBAF1 \cdot u + 0.5 \cdot KBAF2 \cdot u \,|\, u \,|) \hspace{4cm} \text{Equation 6}$$

where u is the gas velocity; Δp is the pressure gradient; KBAF1 is an input constant analogous to Darcy's permeability coefficient k1, and KBAF2 is another input constant analogous to non-Darcy's permeability coefficient k2 in Equation 4. Some details about the input parameters in the modeling are listed in Table 2.

Table 2: Parameters Used in Numerical Simulation

K1	3.89E-14 m^2	K2	3.08E-10 m
KBAF1	2.56E+05 m/s	KBAF2	4.5E+06
Viscosity	1.72E-5 Pa.s	Density	1.23 kg/m^3
Coating Thickness	6.91E-4 m		

The geometric parameters are illustrated in Figure 3. The radius of the baffle is modeled as 0.0215 m, which is same as the radius of the opening in the permeability measurement system. Because of symmetric geometry, only one quarter of the structure was used in the simulation. The entry pressure (Xmin in Figure 3) was modeled as a variable that assumes pressures in the range of those used for the experiment and typically were in the range of 100 to 700 kPa (absolute) corresponding to Pi, and outlet pressure was maintained to be at an atmospheric pressure of 100 kPa corresponding to Po at Xmax in Figure 3. Flow rate Q was calculated by integrating the outlet velocity at Xmax.
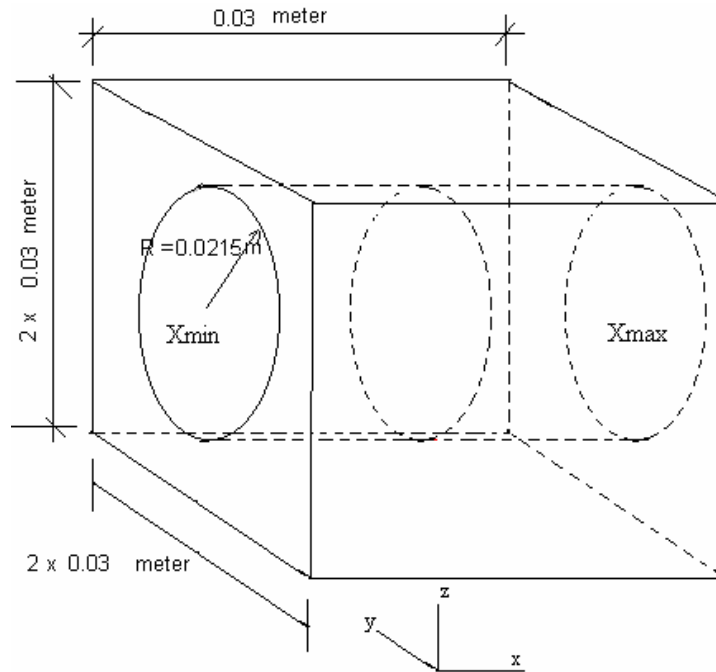
Figure 3. Geometric information in Flow 3D Simulation

RESULTS AND DISCUSSION

Figure 4 shows typical pressure gradient vs. velocity curves at various differential pressures (0 ~ 172 kPa) for the refractory coatings D and E. Darcy's law displayed a clear deviation from the experimental data for both coating D and E. It can be also seen in Figure 4 that Darcy's law underestimates the flow velocity at low-pressure range, while it overestimates the flow velocity at high-pressure range.
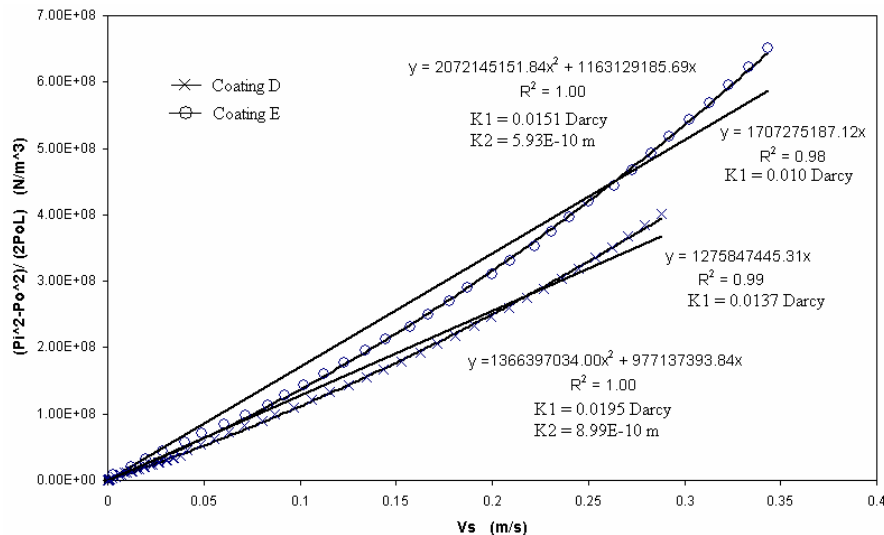

Figure 4: Permeability measurement results of coating D and E (0 ~ 172.37 kPa)

1051

From Figure 5, it can be seen that Darcian permeability coefficient k1 calculated at individual points of the experimental data by Equation 3 will decrease with increasing pressure.[24] It demonstrates the potential of a large discrepancy to predict flow rate at various pressures by using one-point measurement. The pressure gradients vs. velocity curves are parabolic rather than a straight line, which indicates that the inertia has considerable influence in the measurements. By fitting the experimental data to Equation 4, a significant improvement was achieved for both coating D and E when the inertia effects were taken into account, as shown in Figure 4. The values of Darcian permeability coefficients k1 obtained according to different interpretation methods showing large bias in k1 with a large difference of 1.5 times higher for the case when inertia effects were ignored.
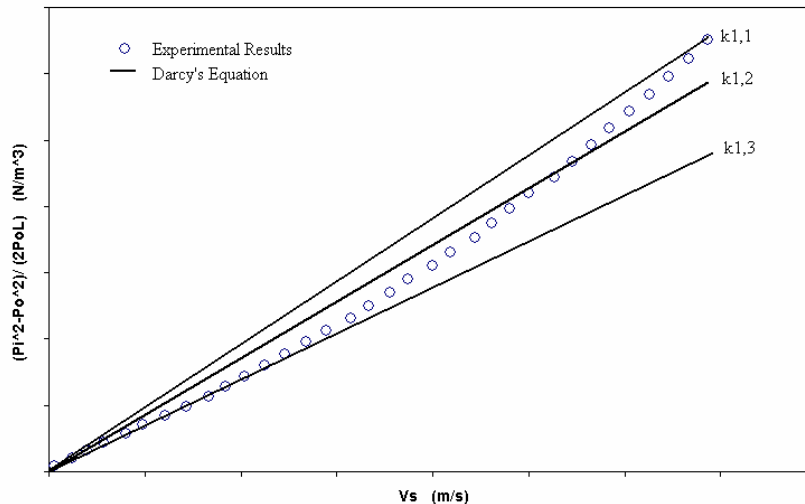

Figure 5. Illustration of Darcian permeability change with velocity

Permeability measurement results for coating A ~ G were shown in Figure 6 and Table 3. Table 3 shows that Forchheimer's equation provided a better fitting (high R2) by considering the inertia effects. The k1 values obtained from Forchheimer's equation were higher than those from the Darcy's law for most of the samples evaluated here. However, the deviation found in Figure 6 and Table 3 were not as significant as observed in Figure 4, which indicates that Darcy's law may still be valid for these coatings in the tested pressure range.
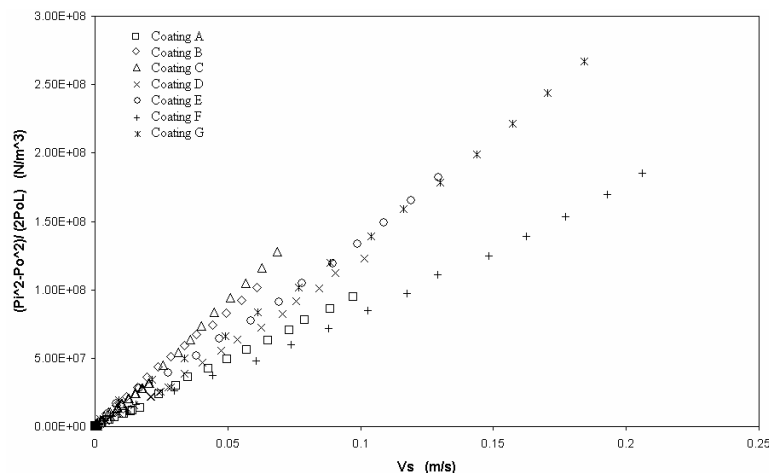

Figure 6: Permeability results of coating A ~ G (0 ~ 68.95 kPa)

Table 2. Permeability Results of Coating A ~ G (0 ~ 68.95 kPa)

Coating	Thickness (cm)	Forchheimer's Equation			Darcy's Equation		Flow Factor
		K1 (Darcy)	K2 (m)	R^2	K (Darcy)	R^2	
A	0.102	0.0181	9.13e-9	0.9990	0.0180	0.9989	0.1775
B	0.091	0.0092	-3.00e-10	0.9995	0.0102	0.9977	0.1011
C	0.071	0.0109	3.03e-10	0.9985	0.0097	0.9959	0.1535
D	0.080	0.0167	6.80e-10	0.9989	0.0148	0.9966	0.2088
E	0.051	0.0134	2.12e-9	0.9979	0.0128	0.9976	0.2627
F	0.050	0.0227	2.24e-9	0.9994	0.0203	0.9982	0.4540
G	0.036	0.0137	1.52e-9	0.9990	0.0125	0.9982	0.3806

Note: 1 Darcy = 9.87 e-13 m^2 Table 3. Permeability Results of Coating A ~ G (0 ~ 68.95 kPa)

However, it also demonstrates the influence of inertia becomes more pronounced and cannot be considered negligible at high velocity. If comparing the Forchheimer's fitting and Darcy's fitting as shown in Figure 7, it is clear that Forchheimer's equation still displayed a better fit to experimental data than Darcy's law for the whole velocity range (analogous to pressure range).
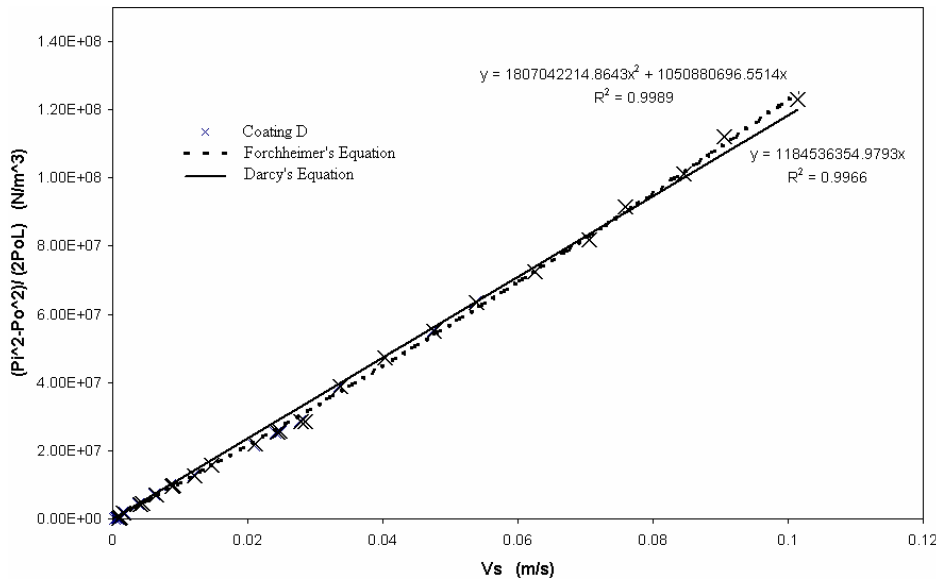

$$y = 1807042214.8643x^2 + 1050880696.5514x$$
$$R^2 = 0.9989$$

$$y = 1184536354.9793x$$
$$R^2 = 0.9966$$

Figure 7: Forchheimer's Equation vs. Darcy's Equation (Coating D 0 ~ 68.95 kPa)

Figure 8 shows the discrepancy of Darcian permeability k1 obtained from Darcy's law and Forchheimer's equation. Darcian permeability k1s obtained from Darcy's law were lower than those calculated by Forchheimer's equation. This effect was also observed in the samples supplied from LFC foundries as shown in Figure 9. This discrepancy became more significant if the Darcian permeability k1 was greater than 0.015 Darcy (1 Darcy = 9.87 e-13 m^2).
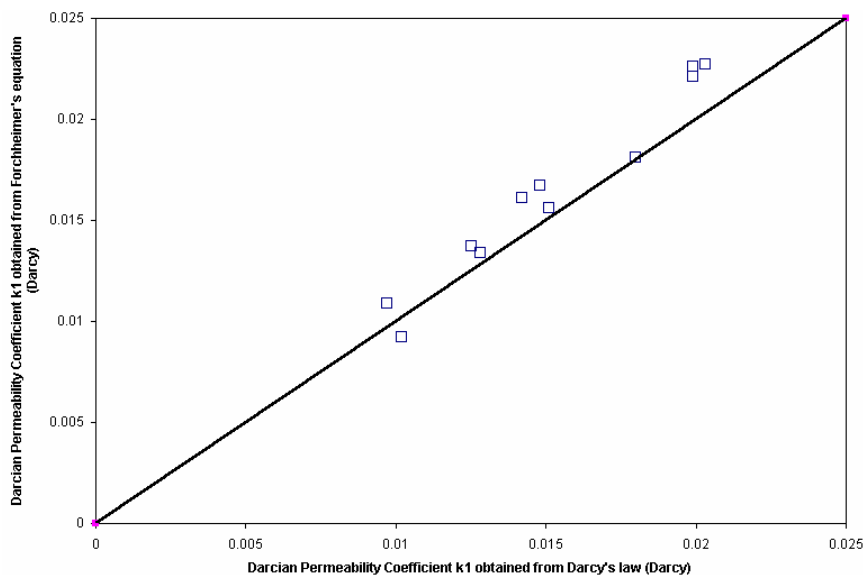
Figure 8: Comparison of k1 obtained from Darcy's Law and Forchheimer's Equation (coating A ~ G, oven dried and temperature dried samples)
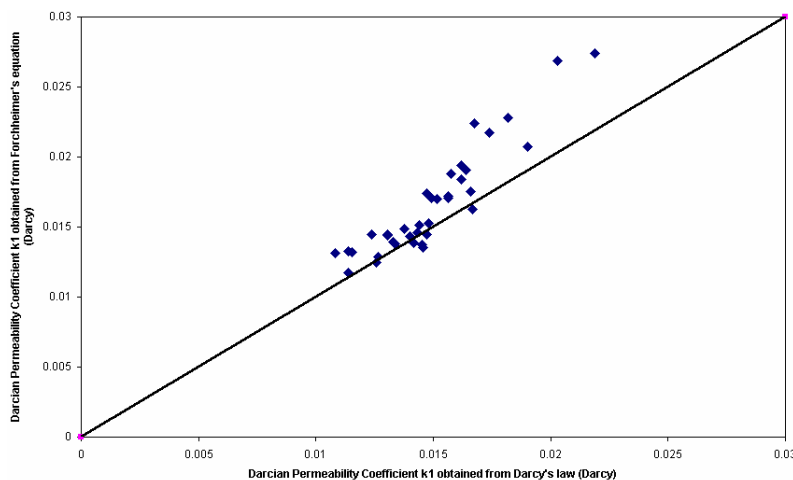

Figure 9: Comparison of k1 Obtained from Darcy's Law and Forchheimer's Equation (Samples supplied by LFC foundries)

If the velocity is controlled to make Re <1, the linear relationship between the pressure gradient and velocity (Darcy's law) may be valid. However, it requires an understanding of a porous medium's microstructure (average pore diameter) to calculate Re according to Equation 5, which is usually unknown and varies from sample to sample. In addition, the calculated permeability coefficients at low velocity (low pressure) cannot be used to predict the flow velocity at other pressures. Figure 10 shows that the Darcian permeability k1 changes with the velocity if one-point measurement is used. The diagram also shows that k1 is extremely high at low velocities (low pressures), which may be caused by the "Klinkenberg effect" in the gas flow. This effect was also observed in other coatings. At low pressures, the gas molecules "slip" in the passages, so the flow velocity will be higher. This effect will become more pronounced when the diameter of the passages is close to the mean free path of the gas molecule,[16] which indicates that characterizing the microstructure of these refractory LFC coatings is also important for understanding the transport properties of these refractory LFC coatings. Research[18] has shown that the Liquid Expulsion Method is very promising to quantify the microstructure of these refractory LFC coatings.
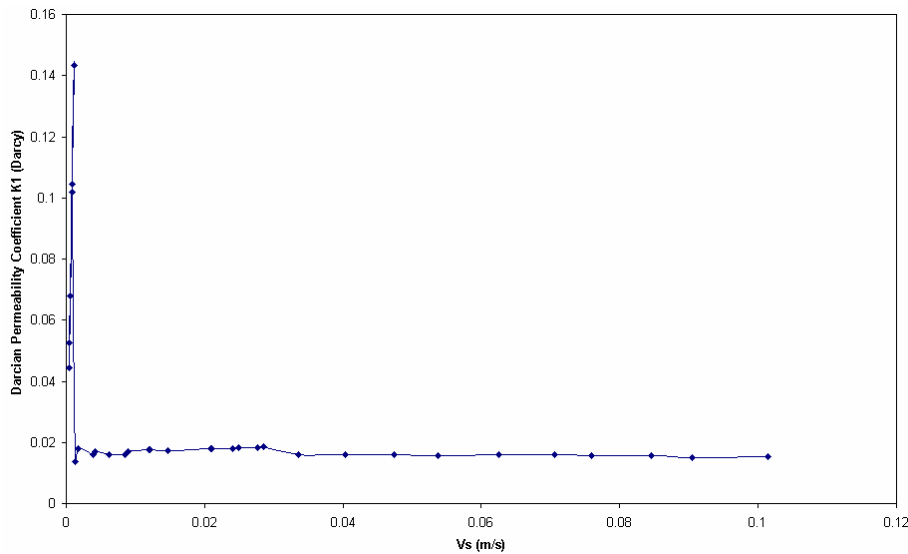
Figure 10: Darcian permeability vs. velocity (coating D 0 ~ 68.95 kPa)

In the FOUNDRY A Perm-meter testing, the coating thickness is not considered in the measurement. However, in order to the get permeability coefficient, the coating thickness must be included in the analysis as seen in Equations 3 and 4. Therefore, the FOUNDRY A Perm-meter readings were normalized (FOUNDRY A Perm-meter reading times coating thickness) to compare with Darcian permeability coefficients k1. Figure 11 shows the linear relationship between the normalized FOUNDRY A Perm-meter reading and k1 obtained from Darcy's law, which indicates that the FOUNDRY A Perm-meter's design is theoretically based on Darcy's law. Figure 11 also shows the large variation of measured results, which may be caused by the one-point measurement in the FOUNDRY A Perm-meter measurement.
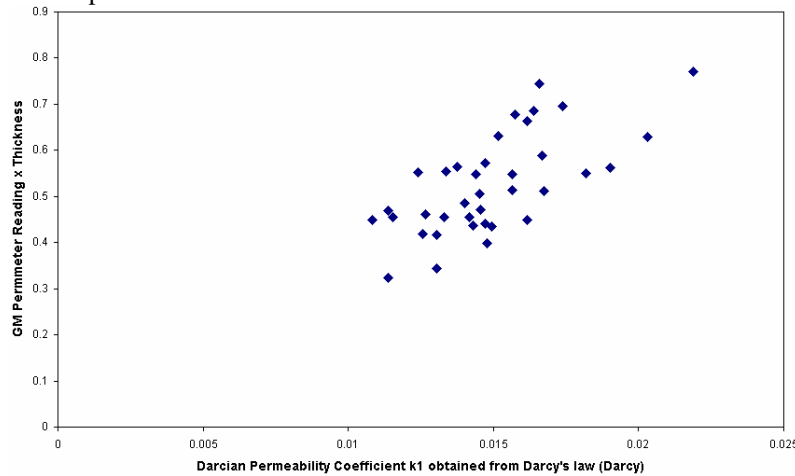

Figure 11: Foundry A Perm-meter results vs. Darcy's Law (samples supplied by LFC foundries)

A similar positive trend was found in Figure 12; however, variation became more significant at large k1, which indicates that inertia effects should not be ignored for high permeable coatings.
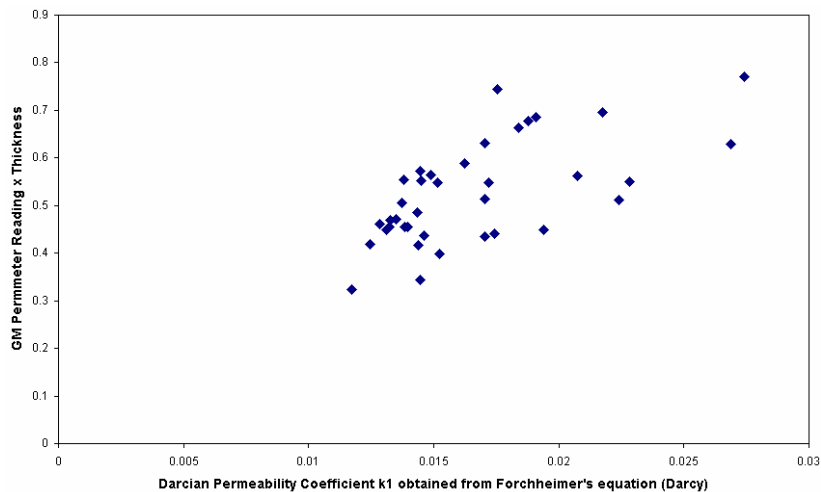
Figure 12: Foundry A Perm-meter results vs. Forchheimer's equation (samples supplied by LFC foundries)

Coating F and G were obtained by diluting coating E and F with 5 percent volume water. From Table 3, it can be seen that coating F has a higher Darcian permeability coefficient k1 than coating D, which indicates the dilution has significant effects on the Coating D. The dilution effects on coating E were not as significant as on coating D. However, dilution reduced coating thickness for both coating D and E. Water dilution is often used in industrial lost foam foundries to work in a target viscosity range, and results indicated above demonstrate that transport properties can be drastically affected depending on coating type, and that this permeability issue needs to be considered for developing control charts.

From Equations 3 and 4, it can be seen that coating thickness is another key factor controlling the coating's transport properties such as permeability coefficient. The term "flow factor" (Darcian permeability coefficient divided by coating thickness) is defined here to normalize the effect of thickness on permeability coefficient(s). This "flow factor" can be used to compare different types of coatings' permeability at the same differential pressure. A Large "flow factor" indicates high permeability of coatings. The "flow factor" listed in Table 3 shows that dilution increased both coating D and E's permeability significantly although it did not affect the permeability coefficients that much, which indicates that thickness is very important to describe the coatings' transport properties. It shows that it is not reasonable to compare the coatings' transport properties by comparing only the permeability coefficients without considering the coatings' thickness. Two coatings having the same permeability coefficients may perform extremely different transport behaviors because of the differences in the coating thickness. The "flow factor," as introduced in this paper, will be able to distinguish these differences by taking the coating thickness into consideration.

Permeability measurement results for oven and room temperature dried samples were shown in Table 4. It can be seen that the oven dry process and the room temperature dry process did not have significantly distinct influences on coating D and E in this study. The differences of coatings D and E between Table 3 and Table 4 can be accounted for in that they were different batches shipped from suppliers.

Table 4: Comparison of Oven and Room Temperature Dry Results

Coating	Thickness	Forchheimer's Equation			Darcy's Equation		Flow Factor
	(cm)	K1	K2	R^2	K	R^2	
		(Darcy)	(m)		(Darcy)		
Oven D	0.053	0.0156	3.7e-9	0.9989	0.0151	0.9987	0.2943
Room D	0.050	0.0161	9.07e-10	0.9986	0.0142	0.9964	0.3220
Oven E	0.051	0.0221	2.01e-9	0.9980	0.0199	0.9951	0.4333
Room E	0.054	0.0226	1.86e-9	0.9989	0.0199	0.9972	0.4185

Note: 1 Darcy = 9.87 e-13 m^2

The relationship between the pressure gradient and velocity for coating D was also investigated in a large differential pressure range (0 ~600 kPa) to emphasize the inertia effects. Figure 13 shows the X direction velocity distribution in the XZ plane, which demonstrates that the X direction velocity is not uniformly distributed.
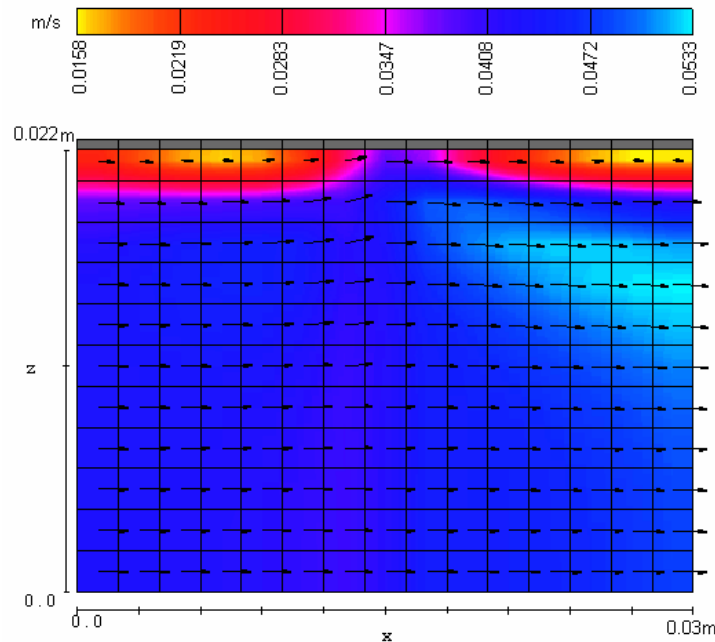

Figure 13: X-Velocity Contour in XZ Plane (Flow3D Simulation)

Figure 14 shows the outlet X direction velocity is a function of the Z coordinate and increases with the increase of applied differential pressures. By integrating the X direction velocity in the Z direction, the overall flow rate through the outlet can be calculated.
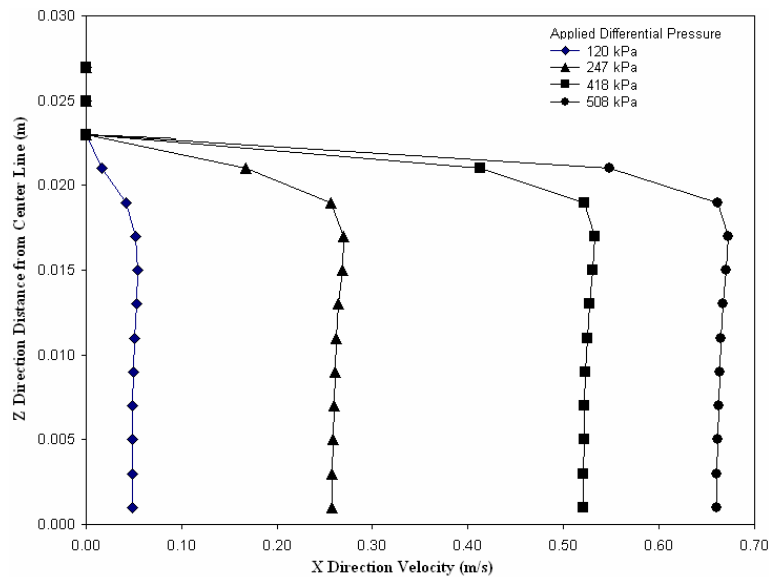
Figure 14: X-velocity vs. Z-coordinate curves (Flow3D Simulation)

Figure 15 shows the good agreement between experimental data and Flow 3D numerical simulation results. Thus, the proposed modeling approach using two experimental calibration parameters obtained from the portable UTK perm-meter system can realistically model the transport properties of gas for a large range of differential pressures. This approach will be a valuable asset for realistic modeling of the refractory coating portion of the boundary value problem involved with LFC using Flow 3D type software.
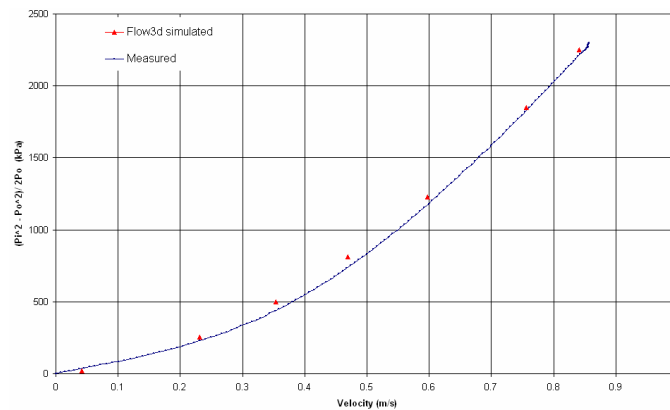
Figure 15: Comparison of measured results with Flow 3D simulation results (0 ~ 586.05 kPa)

CONCLUSIONS

1. A new apparatus for evaluating the permeability of refractory LFC coatings at various pressures was presented that considers the inertia and slippage flow in the analysis of experimental data.
2. This study has shown that Forchheimer's equation is a more realistic model to calculate the permeability coefficients and to predict the LFC refractory coating's transport properties at various pressures.
3. As pressure (velocity) increases, the influences of inertia become more significant and Darcy's law will generate a large discrepancy. Forchheimer's equation should be considered for interpreting the parabolic behavior of the pressure gradient versus velocity curves. At low pressures, the "Klinkenberg effect" may occur. Therefore, special attention should be given for choosing the appropriate pressure range in the permeability measurement.
4. Dilution has different effects on the Darcian permeability coefficient k1. Coating thickness is another key factor to describe the coating transport properties. "Flow factor" is proposed in this research that considers both permeability coefficient(s) and coating thickness.
5. No significant differences were observed in this study for an oven dry process and a room temperature dry process for lost foam casting refractory slurries.
6. The permeability coefficients k1 and k2 obtained from Forchheimer's equation can be effectively modeled in computational fluid dynamics software such as Flow 3D.

ACKNOWLEDGMENTS

REFERENCES

1. S. Shivkumar, X. Yao And M. Makhlouf, *Scripta Metallurgica Et Materialia* **33** (1995) 39.
2. M. Sands And S. Shivkumar, *Journal Of Materials Science* 38 (2003) 2233.
3. C. A. Goria, G. Serramoglia, G. Caironi and G. Tosi, *Transactions Of The American Foundrymen's Society* 94 (1986) 589.
4. M. A. Tschopp, *Transactions Of The American Foundrymen's Society* 110 (2002) 1387
5. M. A. Tschopp, Q. G. Wang And M. J. Dewyse, *Transactions Of The American Foundrymen's Society* 110 (2002) 1371
6. H. Littleton, B. Miller, D. Sheldon and C. Bates, *Foundry Management & Technology* 125 (1997) 41.
7. C. E. Bates, J. A. Griffin and H. E. Littleton, "Expendable Pattern Casting, Casting Defects Manuals" (American Foundrymen's Society, 1994).

8.   S. Bennett, T. Moody, A. Vrieze, M. Jackson, D. R. Askeland and C. W. Ramsay, *Transactions Of The American Foundrymen's Society* 108 (2000) 795

9.   C. Wang, C. W. Ramsay and D. R. Askeland, *Transactions Of The American Foundrymen's Society* 105 (1997) 427.

10.   M. Sands And S. Shivkumar, *Journal Of Materials Science* 38 (2003) 667.

11.   C. H. Tseng And D. R. Askeland, *Transactions of The American Foundrymen's Society* 99 (1991) 455.

12.   C. Ravindran, B. Jue And J. Karpynczyk, *Transactions of The American Foundrymen's Society* 101 (1993) 955

13.   M. J. Lessiter, *Modern Casting* 86 (1996) 45.

14.   L. J. Klinkenberg, In "Drilling And Production Practice", p. 200. American Petroleum Institute, New York, 1941.

15.   P. Forchheimer, *Z. Ver. Deutsch, Ing.* 45 (1901) 1782.

16.   J. Bear, In "Dynamics of Fluids In Porous Media" (American Elsevier Publishing Company, Inc., New York, 1972).

17.   A. E. Scheidegger, In "The Physics Of Flow Through Porous Media" (The Macmillan Company, New York, 1957).

18.   X. Chen And D. Penumadu, *Journal Of Materials Science, 41(11): 3403-3415, (2006).*

19.   D. Penumadu, X. Chen And C. Johnson, *Transactions Of American Foundry Society* Paper No. 04-066 (2004).

20.   R. M. Benson, D. Penumadu, R. Michaels And I. Sen, *Transactions Of American Foundry Society* Paper No. 04-045 (2004).

21.   D. Penumadu, R. Benson And R. Michaels, *Transactions Of American Foundry Society* Paper No. 03-113 (2003).

22.   C. M. Wang, A. J. Paul, W. W. Fincher And O. J. Huey, *Transactions Of American Foundrymen's Society* 101 (1993) 897.

23.   C. W. Hirt and M. R. Barkhudarov, In "Modeling Of Casting, Welding And Advanced Solidification Process VIII Conference", San Diego, California, U.S.A, 1998) P. 51.

24.   M. D. M. Innocentini and V. C. Pandolfelli, *Journal Of American Ceramics Society* 84 (2001) 941.